Continuum Mech. Thermodyn. (2005) 17(4): 311–335
DOI 10.1007/s00161-005-0202-z

ORIGINAL ARTICLE

Alexander N. Gorban · Iliya V. Karlin

Invariance correction to Grad's equations: where to go beyond approximations?

Received: 30 August 2003 / Accepted: 8 April 2005 / Published online: 6 July 2005

Abstract We review some recent developments of Grad's approach to solving the Boltzmann equation and creating a reduced description. The method of the invariant manifold is put forward as a unified principle to establish corrections to Grad's equations. A consistent derivation of regularized Grad's equations in the framework of the method of the invariant manifold is given. A new class of kinetic models to lift the finite-moment description to a kinetic theory in the whole space is established. Relations of Grad's approach to modern mesoscopic integrators such as the entropic lattice Boltzmann method are also discussed.

Keywords Boltzmann equation · Invariant manifolds · Kinetic models · Lattice Boltzmann method · Microflow

PACS 05.20.Dd, 51.10.+y, 47.11.+j

1 Introduction

There has been a long-standing quest to improve on the Grad 13-moment approximation [1]. In particular, such an improvement is needed to study the interplay between hydrodynamics and kinetics in the domain of moderate Knudsen numbers, in particular, simulations of flows at a micrometer scale in so-called micro-electro-mechanical systems (MEMS) [2]. The recent renewed interest in this topic is consistent with the current trend in computational fluid mechanics to use minimal kinetic models instead of more traditional numerical schemes for hydrodynamic equations.

Let us recall the famous Grad's 10-moment and 13-moment approximations for the distribution function:

$$f = f^{(0)}\left\{1 + \frac{1}{p}\boldsymbol{\sigma} : \left(\boldsymbol{cc} - \frac{1}{3}\mathbf{1}c^2\right)\right\}, \tag{1}$$

$$f = f^{(0)}\left\{1 + \frac{1}{p}\boldsymbol{\sigma} : \left(\boldsymbol{cc} - \frac{1}{3}\mathbf{1}c^2\right) + \frac{4}{5pv_T}\boldsymbol{q}\cdot\boldsymbol{c}\left(c^2 - \frac{5}{2}\right)\right\}. \tag{2}$$

Communicated by H. Struchtrup

A. N. Gorban
Department of Mathematics, University of Leicester, LE1 7RH Leicester, UK

I. V. Karlin (✉)
ETH Zürich, Institute of Energy Technology, CH-8092 Zürich, Switzerland
E-mail: karlin@lav.mavt.ethz.ch

Here, as usual, $f^{(0)}$ is the local Maxwellian, $\boldsymbol{c} = v_T^{-1}(\boldsymbol{v} - \boldsymbol{u})$ is the "peculiar" velocity, $\boldsymbol{u}$ is the local flow velocity, $v_T = \sqrt{m/2k_\mathrm{B}T}$ is thermal velocity, p is scalar pressure, $\boldsymbol{\sigma}$ is the nonequilibrium stress tensor, and $\boldsymbol{q}$ is the heat flux,

$$\sigma_{ik}(f) = \int \left[m(v_i - u_i)(v_k - u_k) - \frac{1}{3}\delta_{ik} m\,(\boldsymbol{v} - \boldsymbol{u})^2 \right] f \mathrm{d}\boldsymbol{v},$$

$$q_i(f) = \int \left[\frac{m}{2}(v_i - u_i)\left((\boldsymbol{v} - \boldsymbol{u})^2 - \frac{5k_B T}{m} \right) \right] f \mathrm{d}\boldsymbol{v}.$$

Technically, in Grad's original approach, parametric families (1) and (2) were introduced as truncated Hermite polynomial expansions of the distribution function around local Maxwellians. However, it is much more attractive to view Grad's distributions as parametrically specified sub-manifolds ("surfaces") in the larger space of distribution functions. Grad's method has launched a host of new methods focused around the hard question of nonequilibrium statistical mechanics: how to effectively reduce the microscopic to a macroscopic description? This review is devoted to some selected instances of this question.

2 Grad's method and beyond

"Grad's legacy" (where and how to go beyond the 13-moment approximation) was interpreted and extended in different ways by many authors. Let us mention those which are most relevant to the present discussion.

2.1 Quasi-equilibrium approximation

Quasi-equilibrium approximation (or maximum entropy approximation) in the application to the Boltzmann equation was established in the sixties by several authors, in particular, by Kogan [3] and Lewis [4], though we note that it was already mentioned by Grad himself, and also by Koga (cf. [4]). A detailed discussion of the geometrical aspects of quasi-equilibria was given in [5]. The construction is based on solving the conditional maximization problem. For the concave functional $S = -k_\mathrm{B}\int f \ln f \mathrm{d}\boldsymbol{v}$ (local entropy density) and for given distinguished linear functionals $M(f)$, we find

$$S \to \max,\ M(f) = M. \tag{3}$$

The solution in terms of Lagrange multipliers (dual variables) Λ is written as

$$f = \exp\left\{ \sum_k \Lambda_k D_f M_k \right\}. \tag{4}$$

If $M_k(f) = \int m_k(\boldsymbol{v}) f \mathrm{d}\boldsymbol{v}$, then we have

$$f = \exp\left\{ \sum_k \Lambda_k m_k \right\}. \tag{5}$$

If $M = M_0 = \int\{1, \boldsymbol{v}, v^2\} f \mathrm{d}\boldsymbol{v}$, the parametric set (4) coincides with the set of local Maxwellians. If $M = \int\{1, \boldsymbol{v}, \boldsymbol{v}\boldsymbol{v}\} f \mathrm{d}\boldsymbol{v}$ this is the 10-moment quasi-equilibrium approximation, whose expansion to linear order in $\boldsymbol{\sigma}/p$ coincides with Grad's 10-moment approximation (1). Though almost pedantic, some attention is required when proceeding to the 13-moment case where functions (4) are defined in terms of dual variables. What is not always well defined is the moment chart (or moment parameterization) of these sets, or, $\Lambda(M)$, and a regularization of divergent integrals is required. This can be done either by restricting the velocity integration domain to a large ball $v \le \sqrt{E}$, where E is the total kinetic energy of

the gas in a container [3], or by introducing a higher-order even velocity polynomial (at the price of an extra variable). In the first case of regularization it is possible to use the smallness of $\boldsymbol{q}/pv_T$ to expand the regularized distribution and send the radius of the ball to infinity to end up with the 13-moment Grad's approximation (2).

A particularly useful version of entropic methods was introduced in [6] for chemically reacting gas mixtures, and discussed in some detail for a single-component gas in [7, 8] (triangle entropy method). It can be viewed either as a stepwise realization of the basic maximization problem, or (better) as a self-consistent recipe. Let us split the totality of distinguished macroscopic variables M into M' and M'', where M' are linear functionals for which we can solve explicitly the problem (3) ("easy variables"), and where M'' are "difficult variables". The difficult variables may be even nonlinear in the distribution function, for example scattering rates (see below), so that even the statement of the problem of the entropy maximization can cause difficulties. The triangle entropy method allows construction of quasi-equilibria even in these cases. Let us denote $f(M')$ as the quasi-equilibrium corresponding to the easy variables. Then the triangle quasi-equilibrium for the difficult variables is found by expanding the entropy functional up to quadratic order around $f(M')$, and finding the maximum under the conditions that (i) easy variables M' are not changed, and (ii) difficult variables are fixed to a linear order. That is,

$$\begin{aligned} \Delta S(\delta f) \;&=\; S(f(M')) - k_{\mathrm{B}} \int [\ln f(M') + 1]\delta f \,\mathrm{d}\boldsymbol{v} + \frac{1}{2} k_{\mathrm{B}} \int f(M')^{-1} \delta f^2 \mathrm{d}\boldsymbol{v} \to \max, \\ &\text{(i)}\;\; M'(\delta f) = 0, \\ &\text{(ii)}\;\; D_f M''\big|_{f(M')}(\delta f) = \delta M''. \end{aligned} \tag{6}$$

Maximization here is with respect to δf, nonlinear parametric dependence on M' is not varied. One useful property is that (6) is always solvable in closed form, and the resulting triangle quasi-equilibrium,

$$f(M', \delta M'') = f(M') + \delta f(M', \delta M''), \tag{7}$$

depends linearly on $\delta M''$ and nonlinearly on M' (so the overall dependence is *quasi-linear*). If M' are the five hydrodynamic fields, and if M'' are $\int \boldsymbol{v}\boldsymbol{v} f \,\mathrm{d}\boldsymbol{v}$ or $\int \{\boldsymbol{v}\boldsymbol{v}, \boldsymbol{v}v^2\} f \,\mathrm{d}\boldsymbol{v}$ (both easy and difficult variables are linear in this example), then (7) are Grad's 10- and 13-moment distributions, respectively [7].

The advantage of the quasi-equilibrium approximations is that they are equipped naturally with the thermodynamic parameterization [9]. The structure of the thermodynamic parameterization assumes specification of the projector P onto the tangent bundle of the quasi-equilibrium manifold. For quasi-equilibria, this is (we stick to case (5) for simplicity):

$$PJ = \sum_k \frac{\partial f(M)}{\partial M_k} \int m_k J \, d\boldsymbol{v}. \tag{8}$$

The purpose of projector P is to define dynamics along the manifold. Namely, if we write the Boltzmann equation,

$$D_t f = J(f) = -(\boldsymbol{v} - \boldsymbol{u}) \cdot \nabla f + Q(f, f), \tag{9}$$

where $Q(f, f)$ is the Boltzmann collision integral, and $D_t = \partial_t + \boldsymbol{u} \cdot \nabla$ is the time derivative in the co-moving reference system, then the vector field attached to each state on the quasi-equilibrium manifold (or the microscopic time derivative) is:

$$D_t^{\mathrm{micro}} f(M) = J(f(M)). \tag{10}$$

Here, we simply evaluate the action of the operator on the right hand side of the Boltzmann Eq. (9) on the quasi-equilibrium distributions. On the other hand, under the action of the projector P (8), vectors $J(f(M))$ yield the vector field on the tangent bundle of the quasi-equilibrium manifold, or the macroscopic time derivative:

$$D_t^{\mathrm{macro}} f(M) = PJ(f(M)). \tag{11}$$

The latter can be viewed as a short-hand writing of Grad's equations, which follow from (11) upon multiplication with m_k and integration:

$$\partial_t M_k + \boldsymbol{u} \cdot \nabla M_k = \int m_k P J(f(M))\, \mathrm{d}\boldsymbol{v}. \tag{12}$$

One can ask, what is the use of the microscopic time derivative (10) when only its projected piece, $PJ(f(M))$, contributes finally to Grad's moment Eq. (12)? The answer is that the comparison of the vectors $J(f(M))$ and $PJ(f(M))$ measures how good the closure (12) really is. The difference between $J(f(M))$ and $PJ(f(M))$ is of such a great importance that it deserves a specific name. The defect of invariance (of the quasi-equilibrium approximation) is,

$$\Delta(M) = J(f(M)) - PJ(f(M)). \tag{13}$$

A moment representation of the defect is also useful. If $m_1, \ldots, m_n$ are the distinguished moments, and $m_{n+1}, \ldots$ are the higher-order moments, then the velocity-dependent function is equivalent to the infinite sequence $\Delta_i(M)$ by taking moments of (13):

$$\Delta_i(M) = \begin{cases} 0, & i = 1, \ldots, n \\ \int m_i (J(f(M)) - PJ(f(M)))d\boldsymbol{v}, & i = n+1, \ldots \end{cases} \tag{14}$$

Levermore [10] proved hyperbolicity of maximum entropy approximations. Dual parameterization of quasi-equilibrium manifolds prove to be an advantage in numerical realizations (so-called Legendre integrators, see e.g. [11–13] in the context of polymer dynamics).

The quasi-equilibrium approximations reveal most clearly the time hierarchy assumption behind Grad's approach [3]. In the fast relaxation, the entropy grows according to Boltzmanns equation until maximum of entropy is reached on the quasi-equilibrium states. After that the slow evolution takes place along the manifold of the quasi-equilibrium states. Putting this assumption on trial and, if needed, improving on it is the key in seeking corrections to Grad's approximation. The trial is the deviations away from zero of the defect of invariance (13).

In this section, we reviewed the basic structure of Grad's theory, and indicated that a way beyond a given moment approximation should take into account the defect of its invariance. Before proceeding along this line, let us discuss two other routes, which can be indicated as "increase the number of variables" and "take other variables".

2.2 Many moments approximations

With a given moment approximation at hand, and without asking "how good is this approximation?", there is only one option to try to improve on it - to extend the list of distinguished variables, and to construct another approximation. This viewpoint dominated earlier studies on moment approximations, and was followed by many authors, in particular, by Müller and Ruggeri [14] and their collaborators, mostly in the quasi-linear form, using orthogonal functions developments, and for the Bhatnagar-Gross-Krook model collision integral with phenomenological dependence of the relaxation parameter. Convergence to Boltzmann equation is a difficult question; in fact, it is not expected that Grad's distributions converge to solutions of the Boltzmann equation, even pointwise [15]. On the other hand, as numerical results show [14], the weak convergence (convergence of the moments) can be expected in the linear case. However, without at least evaluating the defect, Eqs. (13) or (14), the uncontrollability of approximations with any number of moments remains.

2.3 Scattering rates as independent variables

Remarkably, Grad's approximations with moments as slow variables (1) and (2) (or any other with more moments) do not contain any molecular information. This shortcoming is inherited from the use of simple

sets of orthogonal functions in the original Grad method. However, if one thinks of using less variables to capture more physics, then other (non-moment) quantities can be tried. In particular, for a pure gas, interesting variables are the scattering rates of moments. For example,

$$\boldsymbol{\sigma}^{\mathrm{coll}} = \int m\boldsymbol{v}\boldsymbol{v}Q(f, f)\,\mathrm{d}\boldsymbol{v} \tag{15}$$

is the scattering rate of the stress tensor, where Q is the Boltzmann collision integral. The variable $\boldsymbol{\sigma}^{\mathrm{coll}}$, unlike $\boldsymbol{\sigma}$, contains information about the molecular interaction. Using the triangle entropy method with the five hydrodynamic variables as easy, and $\boldsymbol{\sigma}^{\mathrm{coll}}$ as difficult (this is indeed the case because $\boldsymbol{\sigma}^{\mathrm{coll}}$ is nonlinear in f), we can construct a "scattering" counterpart of the 10-moment approximation (1):

$$f = f^{(0)}\left\{1 + \frac{1}{p\mu_0(T)}\boldsymbol{\sigma}^{\mathrm{coll}} : \left(\boldsymbol{cc} - \frac{1}{3}\mathbf{1}c^2\right)R(c^2)\right\}, \tag{16}$$

where $\mu_0(T)$ is the first Sonine polynomial approximation to the viscosity coefficient, and the difference from Grad's 10-moment approximation is in the dimensionless function R. The function R depends on the particle's interaction, and R is constant only for Maxwell molecules in which case the present approximation is equivalent to Grad's approximation (up to renaming the variables). For hard spheres [8],

$$R = \frac{5\sqrt{2}}{16}\int_0^1 e^{-c^2t^2}(1 - t^4)(c^2(1 - t^2) + 2)\,\mathrm{d}t. \tag{17}$$

The case for when the scattering rate of the heat flux is included (the counterpart of the 13-moment approximation), and also a mixed version (moments and scattering rates both as distinguished variables), were studied in [7].

Eventually, the triangle entropy method makes it possible to handle "smart" variables which may be more appropriate to the physics of the problem at hand rather then plain moments. The latter assumes a certain degree of a physical intuition; furthermore, the uncontrollability of the resulting quasi-linear quasi-equilibria remains an issue.

2.4 Method of invariant manifold

The general method to derive dynamic corrections on top of successful initial approximations like Grad's was developed by the authors [9, 16–20]. The essence of the method of invariant manifold (MIM) is (i) to write the invariance condition in the differential form (the microscopic time derivative on the manifold equals the macroscopic time derivative), and (ii) to solve this equation by iterations. The choice of the initial approximation is an important problem. Often, it is convenient to start from the quasi-equilibrium manifold (this will be our choice, see below). However, the choice of the initial manifold in MIM is not restricted to quasi-equilibria. The typical example gives us the famous Tamm–Mott-Smith approximation for the strong shock wave (see discussion in [9, 20, 21]). Strictly speaking, the method of invariant manifold can be applied in order to refine any initial approximation compliant with some transversality conditions.

2.4.1 Correction to local Maxwell manifold

In order to explain the two steps of the MIM, we shall consider first, for the purpose of illustration, the invariance correction to the local Maxwell approximation to all orders of Knudsen number.

The main idea is to pose the problem of finding a correction to Euler's hydrodynamics in such a way that Knudsen number expansions do not appear as the necessary element of the analysis. This will be possible by using the Newton method instead of Taylor expansions to get such a correction.

The starting point is the manifold of local Maxwell distribution functions (LM) $f_0(n, \boldsymbol{u}, T; \boldsymbol{v})$, where $\boldsymbol{v}$ is the particle's velocity, and n, $\boldsymbol{u}$, and T are, local number density, average velocity, and temperature

respectively. As is appropriate to our approach, we first check the invariance of the LM manifold. Projector (8) on the LM manifold is:

$$P_0 J = \frac{f_0}{n}\left[\int J\mathrm{d}\boldsymbol{c} + 2\boldsymbol{c}\cdot\int \boldsymbol{c}J\mathrm{d}\boldsymbol{c} + \frac{2}{3}\left(c^2-\frac{3}{2}\right)\int\left(c^2-\frac{3}{2}\right)J\mathrm{d}\boldsymbol{c}\right] \tag{18}$$

By computing the microscopic time derivative (10) on the LM states, projecting it with P_0 (18) to get the macroscopic time derivative (the time derivative due to Euler's equations) (11), and subtracting the second out of the first, we evaluate the invariance defect of the LM manifold (13):

$$\Delta(f_0) = J(f_0) - P_0 J(f_0) = -f_0\left[2\nabla\boldsymbol{u} : \left(\boldsymbol{cc} - \frac{1}{3}\mathrm{I}c^2\right) + v_T\frac{\nabla T}{T}\cdot\boldsymbol{c}\left(c^2-\frac{5}{2}\right)\right]. \tag{19}$$

The defect is not equal to zero as long as their average velocity and the temperature vary in space, as expected. Note that the defect is neither small or large by itself.

To find the correction to the LM manifold, we write the invariance condition as,

$$\Delta(f) = J(f) - PJ(f) = 0, \tag{20}$$

and consider it as an equation to be solved with the initial approximation f_0 for the manifold and P_0 for the projector since both are unknown in (20). This might seem too much to require, however, the well posed nature of the problem is restored once the additional requirement that the manifold we are looking for should be the manifold of slow motions is invoked (see [17] for details). Here we will consider the first iteration.

Upon substitution of P_0 in place of P, and of $f_1 = f_0 + \delta f$ in place of f in Eq. (20), and after the linearization in δf, we get

$$L_{f_0}\delta f + (P_0 - 1)(\boldsymbol{v}-\boldsymbol{u})\cdot\nabla\delta f + \Delta(f_0) = 0, \tag{21}$$

where L_{f_0} is the linearized collision integral (linearization in the local Maxwell state, and we keep indicating the linearization point for reasons to be seen later). Equation (21) has to be solved subject to the condition,

$$P_0\delta f = 0. \tag{22}$$

The linear equation of the first iteration (21) is the most important object in our theory. Indeed, it does not contain the smallness parameter at all, and in fact, was obtained without assumption of a small Knudsen number. If however, the Knudsen number is introduced into Eq. (21) by the usual rescaling,

$$L_{f_0} \to \frac{1}{\epsilon}L_{f_0}, \tag{23}$$

then the first-order in ϵ solution, $\delta f_1 \simeq \epsilon\delta f_1^{(1)}$ is found from the integral equation,

$$L_{f_0}\delta f_1^{(1)} = -\Delta(f_0), \tag{24}$$

which has to be solved subject to the condition $P_0\delta f_1^{(1)}$. It is readily checked that Eq. (24) is just the equation of the first approximation of the Chapman-Enskog method, which is thus recovered as the special case of MIM in the collision-dominated limit.

The invariance equation for the first correction (21) is more complicated than the Chapman-Enskog Eq. (24) because it also contains the spatial derivatives (though it is much *less* complicated than the linearized Boltzmann equation because the there is no time dependence in Eq. (21)). Methods to treat equations of type (20) have also been developed in [16, 17, 20] and worked out for many kinetic systems (not only for the Boltzmann equation). Here we consider, for the purpose of illustration, the small deviations around the global equilibrium in $3D$. We shall treat Eq. (21) in such a way that the Knudsen number will appear explicitly only at the later stages of the computations.

We denote as F_0 the global equilibrium with the equilibrium values of the hydrodynamic quantities, n_0, $\boldsymbol{u}_0 = 0$, and T_0. Deviations are δn, $\delta \boldsymbol{u}$, and δT. We also introduce reduced deviations,

$$\Delta n = \delta n / n_0, \ \ \Delta \boldsymbol{u} = \delta \boldsymbol{u} / v_T^0, \ \Delta T = \delta T / T_0,$$

where v_T^0 is thermal velocity in the equilibrium.

We seek the invariance correction,

$$f_1 = F_0(1 + \varphi_0 + \varphi_1), \tag{25}$$

where

$$\varphi_0 = \Delta n + 2\Delta \boldsymbol{u} \cdot \boldsymbol{c} + \Delta T \left(c^2 - \frac{3}{2} \right). \tag{26}$$

comes from the linearization of the local Maxwellian around F_0, and where φ_1 is the unknown function to be found from equation invariance Eq. (21). In order to find φ_1, we apply a Galerkin approximation in order to achieve a finite-dimensional approximation of the linear collision operator [17], which amounts to setting

$$\varphi_1 = \boldsymbol{A}(\boldsymbol{x}) \cdot \boldsymbol{c} \left(c^2 - \frac{5}{2} \right) + \boldsymbol{B}(\boldsymbol{x}) : \left(\boldsymbol{cc} - \frac{1}{3} I c^2 \right). \tag{27}$$

Our goal is to derive functions $\boldsymbol{A}$ and $\boldsymbol{B}$ from a linearized version of Eq. (21). Knowing $\boldsymbol{A}$ and $\boldsymbol{B}$, we get the following expressions for shear stress tensor $\boldsymbol{\sigma}$ and heat flux vector $\boldsymbol{q}$:

$$\boldsymbol{\sigma} = p_0 \boldsymbol{B}, \ \ \boldsymbol{q} = \frac{5}{4} p_0 v_T^0 \boldsymbol{A}, \tag{28}$$

where p_0 is the equilibrium pressure.

Linearizing Eq. (21) in F_0, substituting φ_1 (27), and switching to the Fourier-transformed in space variables, we derive the set of linear algebraic equations for the Fourier image of the functions $\boldsymbol{A}$ and $\boldsymbol{B}$ (which we denote as $\boldsymbol{a}_k$, and $\boldsymbol{b}_k$, respectively):

$$\begin{gathered} \frac{5 p_0}{3 \mu_0} \boldsymbol{a}_k + i v_T^0 \boldsymbol{b}_k \cdot \boldsymbol{k} = -\frac{5}{2} i v_T^0 \boldsymbol{k} \tau_k, \\ \frac{p_0}{\mu_0} \boldsymbol{b}_k + i v_T^0 \overline{\boldsymbol{k} \boldsymbol{a}_k} = -2 i v_T^0 \overline{\boldsymbol{k} \boldsymbol{\gamma}_k}, \end{gathered} \tag{29}$$

where $i = \sqrt{-1}$, $\boldsymbol{k}$ is a wave vector, μ_0 is the first Sonine polynomial approximation of the shear viscosity coefficient, τ_k and $\boldsymbol{\gamma}_k$ are Fourier images ΔT, and $\Delta \boldsymbol{u}$, respectively, and the over-bar denotes a symmetric traceless dyad.

On introducing the dimensionless reduced wave vector,

$$\boldsymbol{\kappa} = \frac{v_T^0 \mu_0}{p_0} \boldsymbol{k},$$

the solution to Eq. (29) may be written:

$$\begin{aligned} \boldsymbol{b}_k &= -\frac{10 i \overline{\boldsymbol{\gamma}_k \boldsymbol{\kappa}}}{3[(5/3) + (1/2)\kappa^2]} + \frac{5 i (\boldsymbol{\gamma}_k \cdot \boldsymbol{\kappa}) \overline{\boldsymbol{\kappa} \boldsymbol{\kappa}}}{3[(5/3) + (1/2) f^2][5 + 2\kappa^2]} - \frac{15 \tau_k \overline{\boldsymbol{\kappa} \boldsymbol{\kappa}}}{2[5 + 2\kappa^2]}, \\ \boldsymbol{a}_k &= -\frac{15 i \boldsymbol{\kappa} \tau_k}{2[5 + 2\kappa^2]} - \frac{5[\boldsymbol{\kappa} (\boldsymbol{\gamma}_k \cdot \boldsymbol{\kappa}) + \boldsymbol{\gamma}_k f^2 (5 + 2\kappa^2)]}{3[5 + 2\kappa^2][(5/3) + (1/2)\kappa^2]}. \end{aligned} \tag{30}$$

With the Fourier-image of the fluxes (28),

$$\boldsymbol{\sigma}_k = p_0 \boldsymbol{b}_k, \quad \boldsymbol{q} = \frac{5}{4} p_0 v_T^0 \boldsymbol{a}_k,$$

which have to be used to close the Fourier-transformed linear balance equations, functions (30) concludes our computation of the dynamic correction to the linearized local Maxwellian. Note that due to the non-polynomial in κ contributions, the resulting linear hydrodynamics are highly nonlocal. This is, of course, not surprising because no small Knudsen number expansions truncated to some order ever appeared.

Let us briefly consider the new hydrodynamic equations with special attention to the one-dimensional case. Taking the z-axis for the propagation direction, and denoting k_z as k, γ as γ_z, we obtain in (30) the Fourier images of $a = a_z$ and $b = b_{zz}$ (full notation are restored here):

$$a_k = -\frac{\frac{3}{2}p_0^{-1}\mu_0 v_T^0 ik\tau_k + \frac{4}{5}p_0^{-2}\mu_0^2\left(v_T^0\right)^2 k^2\gamma_k}{1+\frac{2}{5}p_0^{-2}\mu_0^2\left(v_T^0\right)^2 k^2},$$
$$b_k = -\frac{\frac{4}{3}p_0^{-1}\mu_0 v_T^0 ik\gamma_k + p_0^{-2}\mu_0^2\left(v_T^0\right)^2 k^2\tau_k}{1+\frac{2}{5}p_0^{-2}\mu_0^2(v_T^0)^2 k^2}. \tag{31}$$

These expressions close the linearized balance equations,

$$\frac{1}{v_T^0}\partial_t \nu_k + ik\gamma_k = 0,$$
$$\frac{2}{v_T^0}\partial_t \gamma_k + ik(\tau_k + \nu_k) + ikb_k = 0, \tag{32}$$
$$\frac{3}{2v_T^0}\partial_t \tau + ik\gamma_k + \frac{5}{4}ika_k = 0.$$

In order to restore the Knudsen number in (31), we introduce $l_{\text{m.f.p.}} = v_T^0\mu_0/p_0$ (the quantity $l_{\text{m.f.p.}}$ is of the order of the mean free path), and we also introduce a hydrodynamic scale l_h, so that $k = \kappa/l_h$, where κ is dimensionless. With this, we obtain in Eq. (31):

$$a_\kappa = -\frac{\frac{3}{2}i\epsilon\kappa\tau_\kappa + \frac{4}{5}\epsilon^2\kappa^2\gamma_\kappa}{1+\frac{2}{5}\epsilon^2\kappa^2},$$
$$b_\kappa = -\frac{\frac{4}{3}i\epsilon\kappa\gamma_\kappa + \epsilon^2\kappa^2\tau_\kappa}{1+\frac{2}{5}\epsilon^2\kappa^2}, \tag{33}$$

where $\epsilon = l_c/l_h$ is the Knudsen number. In the limit $\epsilon \to 0$, Eq. (33) reduces to the familiar Navier-Stokes-Fourier expressions:

$$\sigma_{zz} = -\frac{4}{3}\mu_0\partial_z\delta u_z, \quad q_z = -\lambda_0\partial_z\delta T$$

where $\lambda_0 = 15k_B\mu_0/4m$ is the first Sonine polynomial approximation of the thermal conductivity.

In order to find out a result of non-polynomial behavior (33), it is most informative to calculate a dispersion relation for planar waves. It is worthwhile introducing a dimensionless frequency $\lambda = \omega l_h/v_T^0$, where ω is a complex variable of a wave $\sim \exp(\omega t + ikz)$ (Reω is the damping rate, and Imω is the circular frequency). Making use of (32) and (33), writing $\epsilon = 1$, we obtain the following dispersion relation $\lambda(\kappa)$:

$$12\left(1+\frac{2}{5}\kappa^2\right)^2\lambda^3 + 23\kappa^2\left(1+\frac{2}{5}\kappa^2\right)\lambda^2 + 2\kappa^2\left(5+5\kappa^2+\frac{6}{5}\kappa^4\right)\lambda + \frac{15}{2}\kappa^4\left(1+\frac{2}{5}\kappa^2\right) = 0. \tag{34}$$

Figure 1 presents a dependence Re$\lambda(\kappa^2)$ for acoustic waves obtained from (34) and for the Burnett approximation [15]. The violation in the latter occurs when the curve crosses the horizontal axis. In contrast to the Burnett approximation [15], the acoustic spectrum (34) is stable for all κ. Moreover, Reλ demonstrates a finite limit, as $\kappa \to \infty$ (so-called "Rosenau saturation" [22]).

The example considered demonstrates how to apply the method of the invariant manifold in the simplest case of the initial manifold. Let us now switch back to another case of the initial manifold, the Grad's 13-moment approximation.

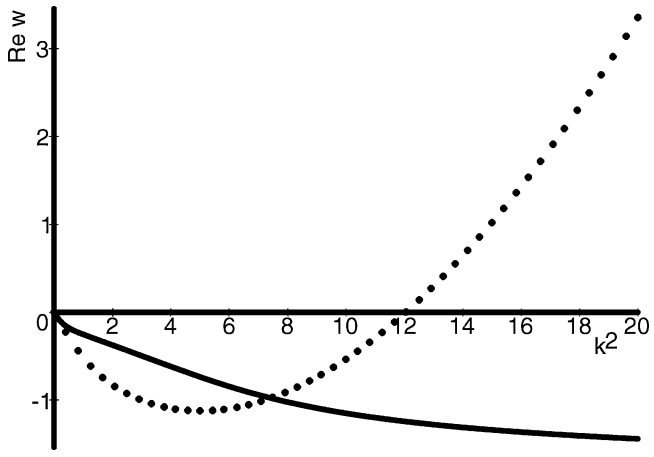

Fig. 1 Attenuation rate of sound waves. Dots are the Burnett approximation. Bobylev's instability occurs when the curve intersects the horizontal axis. Solid line is the first iteration of the Newton method on the invariance equation

2.4.2 Invariance correction to 13-moment manifold

As we said before, MIM is able to address the invariance correction, in principle, to any interesting initial approximation, so it is not surprising that the next candidate after the local Maxwell manifold are manifolds of Grad's distributions. The problem of finding the invariance correction to the moment approximations was first addressed in [23]. Without repeating computations of the [23], our objective here is to explain why the correction to the Grad's manifolds is a distinguished case. Let us start with the quasi-equilibrium of a generic form, and compute the first iteration of the invariance equation,

$$(1-P)L_{f(M)}\delta f + (P-1)(\boldsymbol{v}-\boldsymbol{u})\cdot\nabla\delta f + \Delta(M) = 0, \tag{35}$$

where P is the quasi-equilibrium projector (8), $\Delta(M)$ is the invariance defect of the quasi-equilibrium approximation, and $L_{f(M)}$ is the collision integral, linearized in the quasi-equilibrium. Notice that the latter object is not well studied in the classical theory of the Boltzmann equation, where most of the reduction problems are using the collision integral, linearized in the local equilibrium. A simplification of Eq. (35) happens when we look for Grad's quasi-linear approximations, then, for the linear order accuracy in the higher-order moments, we can replace,

$$L_{f(M)} \to L_{f_0}, \tag{36}$$

in the Eq. (35), where L_{f_0} is the usual linearized collision integral in the local Maxwell state.

Let us proceed further with evaluation of the other terms in the Eq. (35). The projector, corresponding to the 13-moment Grad's approximation, reads,

$$P_{13} = P_0 + \Pi_{13}, \tag{37}$$

where P_0 is the local-equilibrium projector (18), and where Π_{13} acts as follows:

$$\Pi_{13}J = \frac{f_0}{n}\left\{\mathsf{Y} : \int \mathsf{Y}J\,d\boldsymbol{v} + \mathbf{Z}\cdot\int \mathbf{Z}J\,d\boldsymbol{v}\right\}, \tag{38}$$

Here $\mathsf{Y} = \sqrt{2}\overline{\mathbf{cc}}$, and $\mathbf{Z} = \frac{2}{\sqrt{5}}\mathbf{c}(c^2 - \frac{5}{2})$, are peculiar velocity polynomials forming the 13-moment approximation.

Computing the defect of invariance of the 13 moment approximation to the linear order in the φ_{13}, we see, that there are two contributions, the local (containing the linearized collision integral), and the

nonlocal (containing the free flight operator),

$$\begin{aligned}\Delta_{13} &= \Delta_{13}^{\mathrm{loc}} + \Delta_{13}^{\mathrm{nloc}},\\ \Delta_{13}^{\mathrm{loc}} &= (1-\Pi_{13})[L_{f_0} f_0 \varphi_{13}],\\ \Delta_{13}^{\mathrm{nloc}} &= (1-P_{13})[-(\boldsymbol{v}-\boldsymbol{u})\cdot\nabla f_0(1+\varphi_{13})].\end{aligned} \tag{39}$$

Before proceeding any further, we shall discuss the physical significance of the defect (39) because it is the first instance where classical methods, like the Chapman-Enskog method, become inapplicable.

The nonzero defect of invariance of any manifold reveals that the solution to the Boltzmann equation with the initial condition on the manifold leaves this manifold at $t > 0$. The two parts of the defect correspond to two different mechanisms required for this to happen. The local defect is not equal to zero whenever the polynomials Y and $\mathbf{Z}$, forming the Grad manifold, are not eigenvectors of the linearized collision integral. This is distinct from the dynamic noninvariance of local Maxwellians, where in the latter case the local defect is equal to zero whatever the collision model chosen. For the Grad approximation, $\Delta_{13}^{\mathrm{loc}} = 0$ in only two (commonly known) cases, i.e. for Maxwell molecules and for the Bhatnagar-Gross-Krook model (BGK).

It is important to recognize that, whenever the local defect is not equal to zero, the initial manifold has to be *first* corrected locally, in order to bring it closer to the slowest eigenspace of the collision operator, and *before* any nonlocal corrections due to $\Delta_{13}^{\mathrm{nloc}}$ are addressed. It has been demonstrated in [23] that the first local correction to the 13-moment approximation results in Grad's equations corrected in the sense that the transport coefficients become the *exact* Chapman-Enskog coefficients (not the first Sonine polynomial approximation, as in the original Grad equations). Whether or not the local correction is spectacular in the context of the single-component gas with traditional collision models like hard spheres (the first Sonine polynomial approximation is "good" already), the clear distinction between local and nonlocal corrections is crucial. For example, with this distinction it is possible to extend the method of invariant manifolds to driven systems (see the derivation of the Oldroyd constitutive equations from polymer kinetic theory [24]).

Now, let us turn our attention to the nonlocal piece of the defect of invariance. It can be demonstrated that $\Delta_{13}^{\mathrm{nloc}}$ contains no terms with gradients of neither of the five hydrodynamic fields, the only gradient contributing to $\Delta_{13}^{\mathrm{nloc}}$ are of the stress tensor and of the heat flux. In the linear approximation near the global equilibrium F_0 [23],

$$\Delta_{13}^{\mathrm{nloc}} = -v_T^0 F_0(\Pi_{1|krs}\partial_k\sigma_{rs} + \Pi_{2|ik}\overline{\partial_k q_i} + \Pi_3\partial_k q_k), \tag{40}$$

where $\partial_i = \partial/\partial x_i$, and Π are velocity polynomials:

$$\begin{aligned}\Pi_{1|krs} &= c_k\big[c_r c_s - (1/3)\delta_{rs}c^2\big] - (2/5)\delta_{ks}c_r c^2,\\ \Pi_{2|ik} &= (4/5)\big[c^2 - (7/2)\big]\big[c_i c_k - (1/3)\delta_{ik}c^2\big],\\ \Pi_3 &= (4/5)\big[c^2-(5/2)\big]\big[c^2-(3/2)\big] - c^2.\end{aligned}$$

The absence of the gradients of the hydrodynamic fields in the nonlocal defect reveals some important information: the invariance correction to the 13-moment approximation differs from the higher-order corrections to the hydrodynamic equations. For example, since the linearized hydrodynamic equations following from the 13-moment Grad (uncorrected) equations of second order Knudsen number, are the Burnett equations for Maxwell molecules (see for example the comparison of corresponding dispersion relations in [25]), the same is true also for the corrected Grad equations, as explicitly verified by Struchtrup and Torillhon [26].

After this qualitative analysis of the defect of the invariance of Grad's approximation, let us finish setting up the invariance equation of the first iteration formally. With the replacement (36) in the Eq. (35), and using $P_0 L_{f_0} = 0$, we have,

$$(1-\Pi_{13})L_{f_0}\delta f + (P_{13}-1)(\boldsymbol{v}-\boldsymbol{u})\cdot\nabla\delta f + \Delta_{13}^{\mathrm{loc}} + \Delta_{13}^{\mathrm{nloc}} = 0. \tag{41}$$

In principle, this equation can be studied in the same spirit as the equation of the first iteration to local Maxwellians, that is, without introducing small parameters. However, it is much more instructive to consider the collision-dominant case, introducing the scaling (23),

$$(1-\Pi_{13})\frac{1}{\epsilon}L_{f_0}\delta f+(P_{13}-1)(\boldsymbol{v}-\boldsymbol{u})\cdot\nabla\delta f+\frac{1}{\epsilon}\Delta_{13}^{\mathrm{loc}}+\Delta_{13}^{\mathrm{nloc}}=0. \tag{42}$$

The correction δf to first *two orders*, $\delta f\simeq\delta f^{(0)}+\epsilon\delta f^{(1)}$ is found from the equations:

$$(1-\Pi_{13})L_{f_0}\delta f^{(0)}=-\Delta_{13}^{\mathrm{loc}}, \tag{43}$$

$$(1-\Pi_{13})L_{f_0}\delta f^{(1)}=-\Delta_{13}^{\mathrm{nloc}}. \tag{44}$$

These equations have to be solved subject to the additional conditions, $P_{13}\delta f^{(0)}=0$, and $P_{13}\delta f^{(1)}=0$, respectively.

Equation (43) is responsible for the local correction, as expected. It's significance was discussed above. For the following, we assume no local correction is needed, that is, either we assume BGK or Maxwell molecules (then $\delta f^{(0)}=0$), or that the Grad's approximation is a reasonably good approximation for the eigenvectors of L_{f_0}, thus,

$$\delta f^{(1)}=\frac{1}{\tau}\Delta_{13}^{\mathrm{nloc}}. \tag{45}$$

As emphasized in [23], the invariance correction to the 13-moment Grad's approximation is related to the 13-moment Grad equations entirely in the same way as the Navier-Stokes equations are related to the Euler equations. Roughly speaking, it uses the same amount of the Boltzmann collision integral as the classical first-order equation of the Chapman-Enskog method. For that reason, this is the distinguished case among other possible applications of MIM to improve on moment approximations.

2.5 Strongly nonlinear invariance corrections

As we have seen in the previous section, the invariance correction to the quasi-linear quasi-equilibria (Grad's moment approximations) is distinguished by the fact that we can compute it with the usual linearized collision integral in the local equilibrium. The resulting linear integral equations then have the same structure as in the classical Chapman-Enskog method, $L_{f_0}\varphi=\Delta$ (albeit with a different right hand side Δ). The operator L_{f_0} is self-adjoint in the scalar product generated by the second differential of the entropy in the local equilibrium, and thus it is simple to solve. This is not the case when the manifolds we want to correct contain pieces well beyond the vicinity of the local equilibrium, for example, general quasi-equilibria. In these cases, the linearized collision operator $L_{f(M)}$ is not self-adjoint anymore. In such cases, it was suggested to use symmetric linearization in order to establish dynamic corrections in highly nonequilibrium situations. The symmetric linearization of the Boltzmann collision integral in the state f has the form,

$$L_f^{\mathrm{sym}}\delta f=\int w\frac{f'f_1'+ff_1}{2}\left[\frac{\delta f'}{f'}+\frac{\delta f_1'}{f_1'}-\frac{\delta f_1}{f_1}-\frac{\delta f}{f}\right]\mathrm{d}\boldsymbol{v}_1'\mathrm{d}\boldsymbol{v}'\mathrm{d}\boldsymbol{v}_1. \tag{46}$$

Note that $L_f^{\mathrm{sym}}\to L_{f_0}$ if the state f tends to the local Maxwellian f_0 (the consequence of the detail balance, $f'f_1'=ff_1$ in the local equilibrium). Operator L_f^{sym} enjoys the familiar properties of the usual linearized collision integral. Let us introduce notation for the entropic scalar product in the state f. For two distribution functions g_1 and g_2,

$$\langle g_1|g_2\rangle_f=\int\frac{g_1(\boldsymbol{v})g_2(\boldsymbol{v})}{f(\boldsymbol{v})}d\boldsymbol{v}. \tag{47}$$

The following three properties of the operator L_f^{sym} are immediate consequence of the definitions (46) and (47):

(i) $\langle g_1|L_f^{\rm sym}|g_2\rangle_f = \langle g_2|L_f^{\rm sym}|g_1\rangle_f$ (symmetry);
(ii) $\langle g|L_f^{\rm sym}|g\rangle_f \le 0$ (local entropy production inequality);
(iii) $L_f^{\rm sym} g = 0$ if $g/f \in {\rm Lin}\{1, \mathbf{v}, v^2\}$ (conservation laws).

Using the symmetric linearization, we see the equation for the invariance correction for a general quasi-equilibrium $f(M)$ becomes

$$(1-P)L^{\rm sym}_{f(M)}\delta f + (P-1)(\boldsymbol{v}-\boldsymbol{u})\cdot\nabla\delta f + \Delta(M) = 0. \tag{48}$$

The only difference with the Eq. (35) is in the replacement of the linearized collision integral $L_{f(M)}$ with the symmetric linearized collision integral $L^{\rm sym}_{f(M)}$. This difference is crucial though. When using the symmetric operator (46), we get back all the familiar tools for solving integral equations (Fredholm alternative in the collision-dominated case [27] and the parametric expansion without such domination [17] etc). All this is impossible with the plain linearized operator $L_{f(M)}$, for example, even the null-space of $L_{f(M)}$ is not known in general.

The symmetric iteration was tested in the case of finite-dimensional kinetic systems of chemical kinetics [28, 29] (see, in particular, its recent application to the construction of grid representations of invariant manifolds [30]). Results of convergence of symmetric iterations to slow nonlinear manifolds are quite encouraging. At the time of this writing, symmetric iteration remains almost entirely unexplored for the Boltzmann equation.

2.6 Invariance principle in the moment representation

The aforementioned computations of various quasi-equilibria, moment approximations and their invariance corrections were all done in the setting of the kinetic Boltzmann equation and distribution functions. Invariance corrections can also be studied in a simplified setting. Consider a closed system for $n = k+m$ moments and reduce it to a closed system for k of them. Such a simplification (with respect to the full kinetic theory) makes sense especially if one wants to get a basic qualitative understanding about the form of reduced description in terms of k moments.

This problem was studied to some very detailed extend, and well beyond the usual first-order Knudsen number corrections, for the case of hydrodynamics from 10- and 13-moment Grad equations beginning with the paper [7] on a partial summation of the Chapman-Enskog expansion to all the orders in Knudsen number, and on the exact summation of the expansion [31]. Some of these studies were recently summarized in [32] with the emphasis of the iteration method for solving the invariance equation, and the interested reader is directed to that paper. In spite of a seemingly drastic simplification with respect to the "true" kinetic theory, results are sometimes surprisingly robust. For example, the leading invariance correction to the nonlinear longitudinal viscosity in so-called homoenergetic flow found from the 10-moment equations [33] is exactly the one found independently from the exact solution to the model Boltzmann equation [34]. New interesting results on summation of the Chapman-Enskog expansion for the Boltzmann equation were obtained recently by Slemrod [22].

The framework of a larger moment system used to obtain the invariance correction to a smaller moment system appears in the recent work of Struchtrup and Torrilhon [26]. The difference with the derivation from the Boltzmann equation is basically the absence of the local correction. The study [26] demonstrated a set of advantages of these equations above the Grad's system, most importantly, the improved shock wave structure.

3 Quasi-equilibrium kinetic models

The invariance corrections explore more of the phase space than initially assumed by making a Grad approximation with a given number of variables. By measuring the defect of invariance, we realize in which direction the quasi-equilibrium manifold should be improved in order to take into account fast

motion towards it. There is another useful way to explore fast motions by lifting the dynamics from the manifold to a dynamics in the full space by means of a kinetic model.

We recall that lifting the Euler dynamics which takes place on the local Maxwell manifold to a kinetics in the whole phase space is done by the very useful Bhatnagar-Gross-Krook model (BGK),

$$\partial_t f + \boldsymbol{v} \cdot \nabla f = -\frac{1}{\tau}(f - f_0(f)), \tag{49}$$

where $\tau > 0$ is the relaxation time, and $f_0(f)$ is a map $f \to f_0$ established by local conservation laws,

$$\int \{1, \boldsymbol{v}, v^2\}(f - f_0(f))\mathrm{d}\boldsymbol{v} = 0. \tag{50}$$

The right hand side of Eq. (49),

$$Q_{\mathrm{BGK}} = -\frac{1}{\tau}(f - f_0(f)), \tag{51}$$

is called the BGK collision integral. Proof of the H-theorem for the BGK kinetic equation does not rely anymore on the microscopic reversibility (as in the Boltzmann case), instead, it is a simple consequence of convexity of the H-function, and of the property of the map (50):

$$\begin{aligned}\sigma &= -\frac{1}{\tau}\int \ln f(f - f_0(f))\mathrm{d}\boldsymbol{v} \\ &= -\frac{1}{\tau}\int \ln\left(\frac{f}{f_0(f)}\right)(f - f_0(f))\mathrm{d}\boldsymbol{v} \le 0.\end{aligned} \tag{52}$$

Now, how to lift general quasi-equilibria (and, consequently, also the Grad approximations) to a kinetic model? The answer to this question was given in [35]. The kinetic model for a quasi-equilibrium approximation $f(M)$ has the form:

$$\partial_t f + \boldsymbol{v} \cdot \nabla f = -\frac{1}{\tau}(f - f(M(f))) + Q(f(M(f)), f(M(f))). \tag{53}$$

Here $f(M(f))$ is the natural map $f \to f(M)$,

$$\int m_k(f - f(M(f)))\mathrm{d}\boldsymbol{v} = 0,\ k = 1, \ldots, n, \tag{54}$$

and thus the first term in the right hand side of Eq. (53) is just BGK-like, whereas in the second term function $Q(f(M(f)), f(M(f)))$ is the true (Boltzmann) collision integral, evaluated on the quasi-equilibrium manifold. The latter is crucial. Unlike the true Boltzmann collision integral $Q(f, f)$ which can take values in the entire phase space of distribution function, $Q(f(M(f)), f(M(f)))$ is allowed to take values only on a relatively thin subset known a priori, and can be thus pre-computed to the explicit function of M and $\boldsymbol{v}$ (see [35] for examples). If the quasi-equilibrium $f(M)$ consists only of the local Maxwellians, then $Q(f(M(f)), f(M(f)))$ equates to zero, and we get back the BGK-model. In all other cases, the second term in the kinetic model (53) is essential. If it is omitted in Eq. (53) then the zero of the resulting collision integral is the whole quasi-equilibrium manifold $f(M)$, and not its local Maxwellian submanifold, unlike the case of the Boltzmann collision integral.

The H-theorem for kinetic models (53) has the following structure [35], computing σ (52) as:

$$\begin{aligned}\sigma &= \sigma_{\mathrm{BGK}} + \sigma_Q, \\ \sigma_{\mathrm{BGK}} &= -\frac{1}{\tau}\int \ln(f)(f - f(M(f))\mathrm{d}\boldsymbol{v}, \\ \sigma_Q &= \int \ln(f)Q(f(M(f)), f(M(f)))\mathrm{d}\boldsymbol{v}\end{aligned} \tag{55}$$

Function σ_{BGK} is the contribution from the BGK-like term in Eq. (53), and it is always non-positive, again due to the property of the map $f \to f(M)$ (54). The second contribution, σ_Q may be not sign-definite if f is taken far away from the quasi-equilibrium. However, one proves [35] that there always exists a non-empty neighborhood of the quasi-equilibrium manifold, where $\sigma_Q \leq 0$ (this is almost obvious, on the quasi-equilibrium manifold $\sigma_Q(f(M))$ is the entropy production due to the true Boltzmann collision integral). Thus, if the relaxation towards quasi-equilibrium states is fast enough (τ is sufficiently close to zero), the net entropy production inequality holds, $\sigma = \sigma_{\mathrm{BGK}} + \sigma_Q \leq 0$.

Further simplification of the models (53) are possible. Let us mention here two of them. First, instead of the function $Q(f(M(f)), f(M(f)))$, we can use

$$\begin{aligned} PQ(f(M(f)), f(M(f))) &= \sum_k \left.\frac{\partial f(M)}{\partial M_k}\right|_{M=M(f)} R_k(M(f)), \\ R_k(M(f)) &= \int m_k Q(f(M(f)), f(M(f)))d\boldsymbol{v}. \end{aligned} \tag{56}$$

That is, instead of the true collision integral Q, we take only its quasi-equilibrium projection, PQ. The simplification here is that the velocity dependence is now accumulated only in the quasi-equilibrium distribution, and not in the function $Q(f(M(f)), f(M(f)))$:

$$\partial_t f + \boldsymbol{v}\cdot\nabla f = -\frac{1}{\tau}(f - f(M(f))) + \sum_k \left.\frac{\partial f(M)}{\partial M_k}\right|_{M=M(f)} R_k(M(f)). \tag{57}$$

Second, and probably the last simplification if one uses the BGK collision integral Q_{BGK} (51), with a different relaxation time, say θ, instead of the Boltzmann collision integral:

$$\partial_t f + \boldsymbol{v}\cdot\nabla f = -\frac{1}{\tau}(f - f(M(f))) - \frac{1}{\theta}\sum_k \left.\frac{\partial f(M)}{\partial M_k}\right|_{M=M(f)} \left(M_k(f) - M_k^{(0)}(f(M))\right). \tag{58}$$

Here $M_k^{(0)}$ denotes the k-order moment of the local Maxwellian.

As a final comment here, the family of the kinetic models reviewed in this section use the natural map $f \to f(M)$ (54) of the quasi-equilibrium approximations. Different maps $f \to f(M)$ which do not obey (54) were used recently to establish BGK-type models for various quasi-equilibrium approximations [36].

4 Lattice Boltzmann and other minimal kinetic models

The past decade has witnessed a rapid development of *minimal kinetic models* for numerical simulation of complex macroscopic systems. The lattice Boltzmann method is particularly valuable as a minimal extension of the Navier-Stokes equation, and is finding increasing applications in computational fluid dynamics. Some relation of the lattice Boltzmann method to Grad's method was indicated in [37]. Once the Grad method is supplemented by the Gauss-Hermite quadrature in the velocity space, the moment system can be rewritten in the form of a discrete-velocity model, that is, it becomes amenable to effective numerical implementation. Recently, a quasi-equilibrium version of this construction was established, in which the quadrature is done not on the distribution function but on the entropy functional [38, 39]. Quite remarkably, the quasi-equilibrium perspective on the lattice Boltzmann method results in its refinement known as the entropic lattice Boltzmann method [40–42]. Here we review the entropic lattice Boltzmann method (ELBM) for hydrodynamics.

We start with a generic discrete velocity kinetic model. Let $f_i(\boldsymbol{x}, t)$ be populations of the D-dimensional discrete velocities $\boldsymbol{v}_i$, $i = 1, \ldots, n_{\mathrm{d}}$, at position $\boldsymbol{x}$ and time t. The hydrodynamic fields are the linear functions of the populations, namely

$$\sum_{i=1}^{n_{\mathrm{d}}} \left\{1,\ \boldsymbol{v}_i,\ v_i^2\right\} f_i = \{\rho,\ \rho\boldsymbol{u},\ \rho DT + \rho u^2\}, \tag{59}$$

where ρ is the mass density of the fluid, $\rho \boldsymbol{u}$ is the D-dimensional momentum density vector, and $e = \rho DT + \rho u^2$ is the energy density. In the case of isothermal simulations, the set of independent hydrodynamic fields contains only the mass and momentum densities. It is convenient to introduce n_d-dimensional population vectors $\boldsymbol{f}$, and the standard scalar product, $(\boldsymbol{f}|\boldsymbol{g}) = \sum_{i=1}^{n_\mathrm{d}} x_i y_i$. For example, for almost-incompressible hydrodynamics (leaving out the energy conservation), the locally conserved density and momentum density fields are written as

$$(\mathbf{1}|\boldsymbol{f}) = \rho, \ (\boldsymbol{v}_\alpha|\boldsymbol{f}) = \rho u_\alpha. \tag{60}$$

Here $\mathbf{1} = \{1\}_{i=1}^{n_\mathrm{d}}$, $\boldsymbol{v}_\alpha = \{v_{i\alpha}\}_{i=1}^{n_\mathrm{d}}$, and $\alpha = 1, \ldots, D$, where D is the spatial dimension.

The construction of the kinetic simulation scheme begins with finding a convex function of populations H (entropy function), which satisfies the condition that if $\boldsymbol{f}^\mathrm{eq}(\rho, \boldsymbol{u})$ (local equilibrium) minimizes H subject to the hydrodynamic constraints (Eqs. (59) or (60)), then $\boldsymbol{f}^\mathrm{eq}$ also satisfies certain restrictions on the higher-order moments. For example, the equilibrium stress tensor must respect the Galilean invariance,

$$\sum_{i=1}^{n_\mathrm{d}} v_{i\alpha} v_{i\beta} f_i^\mathrm{eq}(\rho, \boldsymbol{u}) = \rho c_\mathrm{s}^2 \delta_{\alpha\beta} + \rho u_\alpha u_\beta. \tag{61}$$

The corresponding entropy functions for the isothermal and the thermal models were found in [39, 41, 43, 44], and are given below (see Sect. 4.3.1 and Table 1). For the time being, assume that the convex function H is given.

The next step is to obtain the set of kinetic equations,

$$\partial_t f_i + v_{i\alpha} \partial_\alpha f_i = \Delta_i. \tag{62}$$

Let $\boldsymbol{m}_1, \ldots, \boldsymbol{m}_{n_\mathrm{c}}$ be the n_d-dimensional vectors of locally conserved fields, $M_i = (\boldsymbol{m}_i|\boldsymbol{f})$, $i = 1, \ldots, n_\mathrm{c}$, $n_\mathrm{c} < n_\mathrm{d}$. The n_d-dimensional vector function $\boldsymbol{\Delta}$ (collision integral), must satisfy the conditions:

$$\begin{aligned} &(\boldsymbol{m}_i|\boldsymbol{\Delta}) = 0, \ i = 1, \ldots, n_\mathrm{c} \text{ (local conservation laws)}, \\ &(\nabla H|\boldsymbol{\Delta}) \le 0 \text{ (entropy production inequality)}, \end{aligned}$$

where ∇H is the row-vector of partial derivatives $\partial H/\partial f_i$. Moreover, the local equilibrium vector $\boldsymbol{f}^\mathrm{eq}$ must be the only zero point of $\boldsymbol{\Delta}$, that is, $\boldsymbol{\Delta}(\boldsymbol{f}^\mathrm{eq}) = \mathbf{0}$, and, finally, $\boldsymbol{f}^\mathrm{eq}$ must be the only zero point of the local entropy production, $\sigma(\boldsymbol{f}^\mathrm{eq}) = 0$. Collision integrals which satisfies all these requirements are called admissible. Let us discuss several possibilities of constructing admissible collision integrals.

4.1 BGK model

Suppose that the entropy function H is known. If, in addition, the local equilibrium is also known as an explicit function of the locally conserved variables (or some reliable approximation of this function is known), the simplest option is to use the Bhatnagar-Gross-Krook (BGK) model. In the case of isothermal hydrodynamics, for example, we write

$$\boldsymbol{\Delta} = -\frac{1}{\tau}(\boldsymbol{f} - \boldsymbol{f}^\mathrm{eq}(\rho(\boldsymbol{f}), \boldsymbol{u}(\boldsymbol{f}))). \tag{63}$$

The BGK collision operator is sufficient for many applications. However, it becomes advantageous only if the local equilibrium is known in a closed form. Unfortunately, often only the entropy function is known but not its minimizer. For these cases one should construct collision integrals based solely on the knowledge of the entropy function. We present here two particular realizations of the collision integral based on the knowledge of the entropy function only.

4.2 Quasi-chemical model

For a generic case of n_c locally conserved fields, let $\boldsymbol{g}_s$, $s = 1, \ldots, n_d - n_c$, be a basis of the subspace orthogonal (in the standard scalar product) to the vectors of the conservation laws. For each vector $\boldsymbol{g}_s$, we define a decomposition $\boldsymbol{g}_s = \boldsymbol{g}_s^+ - \boldsymbol{g}_s^-$, where all components of vectors $\boldsymbol{g}_s^\pm$ are nonnegative, and if $g_{si}^\pm \neq 0$, then $g_{si}^\mp = 0$. Let us consider the collision integral of the form:

$$\boldsymbol{\Delta} = \sum_{s=1}^{n_d - n_c} w_s \boldsymbol{g}_s \{\exp((\nabla H | \boldsymbol{g}_s^-)) - \exp((\nabla H | \boldsymbol{g}_s^+))\}. \tag{64}$$

Here $w_s > 0$. By construction, the collision integral (64) is admissible. If the entropy function is Boltzmann–like, and the components of the vectors $\boldsymbol{g}_s$ are integers, the collision integral assumes the familiar Boltzmann–like form.

4.3 Single relaxation time gradient model

The BGK collision integral (63) has the important property that the linearization of the operator (63) around the local equilibrium point has a very simple spectrum $\{0, -1/\tau\}$, where 0 is the n_c-times degenerate eigenvalue corresponding to the conservation laws, while the non-zero eigenvalue corresponds to the rest of the (kinetic) eigenvectors. Nonlinear collision operators which have this property of their linearizations at equilibrium are called single relaxation time models (SRTM). They play an important role in modelling because they allow for the simplest identification of transport coefficients.

The SRTM, based on the given entropy function H, is constructed as follows (single relaxation time gradient model, SRTGM). For the system with n_c local conservation laws, let $\boldsymbol{e}_s$, $s = 1, \ldots, n_d - n_c$, be an orthonormal basis in the kinetic subspace, $(\boldsymbol{m}_i | \boldsymbol{e}_s) = 0$, and $(\boldsymbol{e}_s | \boldsymbol{e}_p) = \delta_{sp}$. Then the single relaxation time gradient model is

$$\boldsymbol{\Delta} = -\frac{1}{\tau} \sum_{s,p=1}^{n_d - n_c} \boldsymbol{e}_s K_{sp}(\boldsymbol{f})(\boldsymbol{e}_p | \nabla H), \tag{65}$$

where K_{sp} are elements of a positive definite $(n_d - n_c) \times (n_d - n_c)$ matrix $\boldsymbol{K}$,

$$\begin{aligned} \boldsymbol{K}(\boldsymbol{f}) &= \boldsymbol{C}^{-1}(\boldsymbol{f}), \\ C_{sp}(\boldsymbol{f}) &= (\boldsymbol{e}_s | \nabla\nabla H(\boldsymbol{f}) | \boldsymbol{e}_p). \end{aligned} \tag{66}$$

Here, $\nabla\nabla H(\boldsymbol{f})$ is the $n_d \times n_d$ matrix of second derivatives, $\partial^2 H / \partial f_i \partial f_j$. Linearization of the collision integral at equilibrium has the form,

$$\boldsymbol{L} = -\frac{1}{\tau} \sum_{s=1}^{n_d - n_c} \boldsymbol{e}_s \boldsymbol{e}_s, \tag{67}$$

which is obviously single relaxation time. Use of the SRTGM instead of the BGK model results in the same hydrodynamics even when the local equilibrium is not known in a closed form. Further details of this model and its numerical implementation can be found in [39].

It is pertinent to our discussion to explain the term "gradient" appearing in the name SRTGM. In euclidean spaces with the given scalar product, we often identify the differential of a function $f(x)$ with its gradient. In the orthogonal coordinate system $(\mathrm{grad} f(x))_i = \partial f(x) / \partial x_i$. However, when dealing with a more general setting, one can run into problems while making sense out of such a definition. What to do if there is no distinguished scalar product, no preselected orthogonality?

For a given scalar product $\langle \, | \, \rangle$ the gradient $\mathrm{grad}_x f(x)$ of a function $f(x)$ at a point x is such a vector g that $\langle g | y \rangle = D_x f(y)$ for any vector y, where $D_x f$ is the differential of function f at a point x. The differential of function f is the linear functional that provides the best linear approximation near the given point.

In order to transform a vector into a linear functional one needs a pairing, that means a bilinear form $\langle\,|\,\rangle$. This pairing transforms vector g into linear functional $\langle g|$: $\langle g|(x) = \langle g|x\rangle$. Any twice differentiable function $f(x)$ generates a field of pairings i.e., at any point x there exists a second differential of f, a quadratic form $(D_x^2 f)(\Delta x, \Delta x)$. For a convex function these forms are positively definite, and we return to the concept of scalar product. Let us calculate a gradient of f using this scalar product. In coordinate representation the identity $\langle \mathrm{grad} f(x) \mid y\rangle_x = (D_x f)(y)$ (for any vector y) has a form

$$\sum_{i,j} (\mathrm{grad} f(x))_i \frac{\partial^2 f}{\partial x_i \partial x_j} y_j = \sum_i \frac{\partial f}{\partial x_j} y_j, \tag{68}$$

hence,

$$(\mathrm{grad} f(x))_i = \sum_j \left(D_x^2 f\right)^{-1}_{ij} \frac{\partial f}{\partial x_j}. \tag{69}$$

As we can see, this $\mathrm{grad} f(x)$ is the Newtonian direction, and with this gradient the method of steepest descent transforms into the Newton method of optimization.

Entropy is the concave function, and we define the entropic scalar product through negative second differential of entropy. Let us define the gradient of entropy by means of this scalar product: $\langle \mathrm{grad}_x S|z\rangle_x = (D_x S)(z)$. The entropic gradient system is

$$\frac{dx}{dt} = \varphi(x)\mathrm{grad}_x S, \tag{70}$$

where $\varphi(x) > 0$ is a positive kinetic multiplier. The entropic gradient models (70) possesses all the required properties (if the entropy Hessian is sufficiently simple). In many cases it is simpler than the BGK model, because the gradient model is local in the sense that it uses only the entropy function and its derivatives at a current state, and it is not necessary to compute the equilibrium (or quasi-equilibrium for quasi-equilibrium models). The entropic gradient model has a one-point relaxation spectrum, because near the equilibrium x^{eq} the gradient vector field (70) has an extremely simple linear approximation: $d(\Delta x)/dt = -\varphi(x^{\mathrm{eq}})\Delta x$. It corresponds to a well-known fact that the Newton method minimizes a positively defined quadratic form in one step. The SRTGM discrete velocity model (65), (66) is a particular realization of this construction when the local conservation laws are projected out.

4.3.1 H-functions of minimal kinetic models

The Boltzmann entropy function written in terms of the one-particle distribution function $f(\boldsymbol{x}, \boldsymbol{v})$ is $H = \int f \ln f \, d\boldsymbol{v}$, where $\boldsymbol{v}$ is the continuous velocity. Close to the global (reference) equilibrium, this integral can be approximated by using the Gauss–Hermite quadrature with the weight

$$W = (2\pi T_0)^{(D/2)} \exp(-v^2/(2T_0)).$$

Here D is the spatial dimension, T_0 is the reference temperature, while the particles mass and Boltzmann's constant k_{B} are set equal to one. This gives the entropy functions of the discrete-velocity models [41, 43, 44],

$$H = \sum_{i=1}^{n_{\mathrm{d}}} f_i \ln\left(\frac{f_i}{w_i}\right). \tag{71}$$

Here, w_i is the weight associated with the i-th discrete velocity $\boldsymbol{v}_i$ (zeroes of the Hermite polynomials). The discrete-velocity distribution functions (populations) $f_i(\boldsymbol{x})$ are related to the values of the continuous distribution function at the nodes of the quadrature by the formula,

$$f_i(\boldsymbol{x}) = w_i(2\pi T_0)^{(D/2)} \exp\left(v_i^2/(2T_0)\right) f(\boldsymbol{x}, \boldsymbol{v}_i).$$

The entropy functions (71) for various $\{w_i, \boldsymbol{v}_i\}$ are the only input needed for the construction of minimal kinetic models.

With the increase of the order of the Hermite polynomials used in evaluation of the quadrature (71), a better approximation to the hydrodynamics is obtained. The first few models of this sequence are represented in Table 1.

Table 1 Minimal kinetic models [44]

1. Order	2. Fields	3. Velocities	4. Weights	5. Hydrodynamic limit
2	ρ	$\sqrt{T_0}$	1/2	Diffusion
		$-\sqrt{T_0}$	1/2	
3	ρ, $\rho\boldsymbol{u}$	0	2/3	Isothermal Navier–Stokes
		$\sqrt{3}\sqrt{T_0}$	1/6	
		$-\sqrt{3}\sqrt{T_0}$	1/6	
4	ρ, $\rho\boldsymbol{u}$, e	$\sqrt{3-\sqrt{6}}\sqrt{T_0}$	$1/[4(3-\sqrt{6})]$	Thermal Navier-Stokes
		$-\sqrt{3-\sqrt{6}}\sqrt{T_0}$	$1/[4(3-\sqrt{6})]$	
		$\sqrt{3+\sqrt{6}}\sqrt{T_0}$	$1/[4(3+\sqrt{6})]$	
		$-\sqrt{3+\sqrt{6}}\sqrt{T_0}$	$1/[4(3+\sqrt{6})]$	

Column 1: order of Hermite velocity polynomial used to evaluate the Gauss-Hermite quadrature; Column 2: locally conserved (hydrodynamic) fields; Column 3: discrete velocities for $D = 1$ (zeroes of the corresponding Hermite polynomials). For $D > 1$, discrete velocities are all possible tensor products of the one-dimensional velocities in each component direction; Column 4: weights in the entropy formula (71), corresponding to the discrete velocities of the Column 3. For $D > 1$, the weights of the discrete velocities are products of corresponding one-dimensional weights; Column 5: macroscopic equations for the fields of Column 2 recovered in the hydrodynamic limit of the model.

4.4 Entropic lattice Boltzmann method

If the set of discrete velocities forms the links of a Bravais lattice (with possibly several sub-lattices), then the discretization of the discrete velocity kinetic equations in time and space is particularly simple, and leads to the entropic lattice Boltzmann scheme. This happens in the important case of the isothermal hydrodynamics. The equation of the entropic lattice Boltzmann scheme reads as,

$$f_i(\boldsymbol{x} + \boldsymbol{c}_i\delta t, t + \delta t) - f_i(\boldsymbol{x}, t) = \beta\alpha(\boldsymbol{f}(\boldsymbol{x}, t))\Delta_i(\boldsymbol{f}(\boldsymbol{x}, t)), \tag{72}$$

where δt is the discretization time step, and $\beta \in [0, 1]$ is a fixed parameter which matches the viscosity coefficient in the long-time large-scale dynamics of the kinetic scheme (72). The function α of the population vector defines the maximal over-relaxation of the scheme, and is found from the entropy condition,

$$H(\boldsymbol{f}(\boldsymbol{x}, t) + \alpha\boldsymbol{\Delta}(\boldsymbol{f}(\boldsymbol{x}, t)) = H(\boldsymbol{f}(\boldsymbol{x}, t)). \tag{73}$$

The nontrivial root of this equation is found for populations at each lattice site. Eq. (73) ensures the discrete-time H-theorem, and is required in order to stabilize the scheme if the relaxation parameter β is close to one. The geometrical sense of the discrete-time H-theorem is explained in Fig. 2. We note in passing that the latter limit is of particular importance in the applications of the entropic lattice Boltzmann method to hydrodynamics because it corresponds to vanishing viscosity, and hence to numerically stable simulations of very high Reynolds number flows.

4.5 Entropic lattice BGK method (ELBGK)

An important simplification occurs in the case of the isothermal simulations when the entropy function is constructed using third-order Hermite polynomials (see Table 1): the local equilibrium population vector can be obtained in closed form [44]. This enables the simplest entropic scheme – the entropic lattice BGK model – for simulations of isothermal hydrodynamics. We present this model in dimensionless lattice units.

Let D be the spatial dimension. For $D = 1$, the three discrete velocities are

$$\boldsymbol{v} = \{-1, 0, 1\}. \tag{74}$$

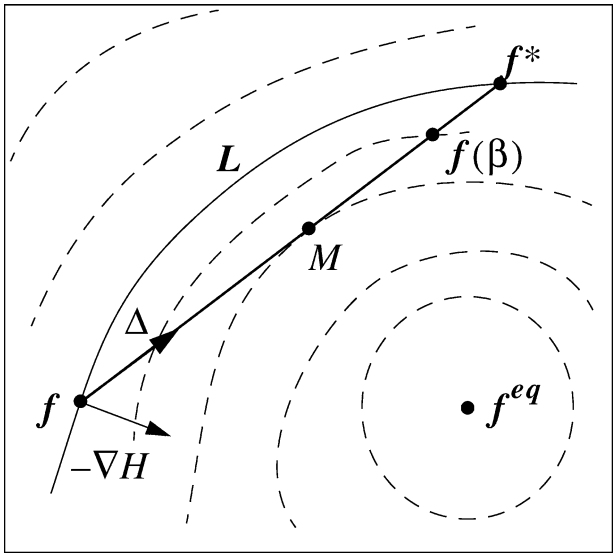

Fig. 2 Entropic stabilization of the lattice Boltzmann scheme with over-relaxation. Curves represent entropy levels, surrounding the local equilibrium f^{eq}. The solid curve L is the entropy level with the value $H(f) = H(f^*)$, where f is the initial, and f^* is the maximally over-relaxed population $f + \alpha\Delta$ defined by Eq. (73). The vector Δ represents the collision integral, the sharp angle between Δ and the vector $-\nabla H$ reflects the entropy production inequality. The point M is the state of minimum of the entropy function H on the line segment between f and f^*. The result of the collision update is represented by the point $f(\beta)$. The choice of β shown corresponds to the over-relaxation: $H(f(\beta)) > H(M)$ but $H(f(\beta)) < H(f)$. The particular case of the BGK collision (not shown) would be represented by a vector Δ_{BGK}, pointing from f towards f^{eq}, in which case $M = f^{\mathrm{eq}}$. Figure from [41]

For $D > 1$, the discrete velocities are tensor products of the discrete velocities of these one-dimensional velocities. Thus, we have the 9-velocity model for $D = 2$ and the 27-velocity model for $D = 3$. The H function is Boltzmann-like:

$$H = \sum_{i=1}^{3^D} f_i \ln\left(\frac{f_i}{w_i}\right). \tag{75}$$

The weights w_i are associated with the corresponding discrete velocity $\boldsymbol{v}_i$. For $D = 1$, the three-dimensional vector of the weights corresponding to the velocities (74) is

$$\boldsymbol{w} = \left\{\frac{1}{6}, \quad \frac{2}{3}, \quad \frac{1}{6}\right\}. \tag{76}$$

For $D > 1$, the weights are constructed by multiplying the weights associated with each component direction.

The local equilibrium minimizes the H-function (71) subject to the fixed density and momentum,

$$\sum_{i=1}^{3^D} f_i = \rho, \quad \sum_{i=1}^{3^D} f_i v_{i\alpha} = \rho u_\alpha, \quad \alpha = 1, \ldots, D. \tag{77}$$

The explicit solution to this minimization problem reads,

$$f_i^{\mathrm{eq}} = \rho w_i \prod_{\alpha=1}^{D} \left(2 - \sqrt{1 + 3u_\alpha^2}\right) \left(\frac{2\,u_\alpha + \sqrt{1 + 3\,u_\alpha^2}}{1 - u_\alpha}\right)^{c_{i\alpha}}. \tag{78}$$

Note that the exponent, $v_{i\alpha}$, in (78) takes the values ± 1, and 0 only, and the speed of sound, c_s, in this model is equal to $1/\sqrt{3}$. The factorization of the local equilibrium (78) over spatial components is quite remarkable, and resembles the familiar property of the local Maxwellians.

The entropic lattice BGK model for the local equilibrium (78) reads,

$$f_i(\boldsymbol{x} + \boldsymbol{v}_i\delta t, t + \delta t) - f_i(\boldsymbol{x}, t) = -\beta\alpha(f_i(\boldsymbol{x}, t) - f_i^{\mathrm{eq}}(\rho(\boldsymbol{f}(\boldsymbol{x}, t)), \boldsymbol{u}(\boldsymbol{f}(\boldsymbol{x}, t)))). \tag{79}$$

The parameter β is related to the relaxation time τ of the BGK model (63) by the formula,

$$\beta = \frac{\delta t}{2\tau + \delta t}, \tag{80}$$

and the value of the over-relaxation parameter α is computed at each lattice site from the entropy estimate,

$$H(\boldsymbol{f} - \alpha(\boldsymbol{f} - \boldsymbol{f}^{\mathrm{eq}}(\boldsymbol{f}))) = H(\boldsymbol{f}). \tag{81}$$

In the hydrodynamic limit, the model (79) reconstructs the Navier-Stokes equations with the viscosity

$$\mu = \rho c_s^2 \tau = \rho c_s^2 \delta t \left(\frac{1}{2\beta} - \frac{1}{2}\right). \tag{82}$$

The zero-viscosity limit corresponds to $\beta \to 1$.

4.6 Wall boundary conditions

The boundary (a solid wall) ∂R is specified at any point $\boldsymbol{x} \in \partial R$ by the inward unit normal $\boldsymbol{e}$, the wall temperature T_{wall}, and the wall velocity $\boldsymbol{u}_{\mathrm{wall}}$. The simplest boundary condition for the minimal kinetic models presented above is obtained upon evaluation of the diffusive wall boundary condition for the Boltzmann equation [45] with the help of the Gauss-Hermite quadrature. Details can be found in [43, 46]. We here write out the final expression for the diffusive wall boundary condition:

$$f_i = \frac{\sum_{\xi_{i'}\cdot\boldsymbol{n}<0} |(\boldsymbol{\xi}_{i'} \cdot \boldsymbol{n})| f_{i'}}{\sum_{\xi_{i'}\cdot\boldsymbol{n}<0} |(\boldsymbol{\xi}_{i'} \cdot \boldsymbol{n})| f_{i'}^{\mathrm{eq}}(\rho_{\mathrm{wall}}, \boldsymbol{u}_{\mathrm{wall}})} f_i^{\mathrm{eq}}(\rho_{\mathrm{wall}}, \boldsymbol{u}_{\mathrm{wall}}), \quad (\boldsymbol{\xi}_i \cdot \boldsymbol{n} > 0). \tag{83}$$

Here $\boldsymbol{\xi}_i$ is the discrete velocity in the wall reference frame, $\boldsymbol{\xi}_i = \boldsymbol{v}_i - \boldsymbol{u}_{\mathrm{wall}}$.

4.7 Numerical illustrations of the ELBGK

The Kramers problem [45] is a limiting case of the plane Couette flow, where one of the plates is moved to infinity, while keeping a fixed shear rate. The analytical solution for the slip-velocity at the wall calculated for the linearized BGK collision model [45] with the simulation of the entropic lattice BGK model are compared in Fig. 3. This shows that one important feature of the original Boltzmann equation, the Knudsen number dependent slip at the wall, is retained in the present model.

In another numerical experiment, the ELBGK method was tested in the setup of the two-dimensional Poiseuille flow. The time evolution of the computed profile as compared to the analytical result obtained from the incompressible Navier–Stokes equations is demonstrated in Fig. 4.

The entropic lattice Boltzmann method upgrades the standard lattice BGK scheme [47] to efficient, accurate, and unconditionally stable simulation algorithm for high Reynolds number flows [48, 49]. As an illustration, we present the result of comparison of the entropic lattice Boltzmann scheme versus the accurate spectral element code in the setup of the freely decaying two-dimensional turbulence, see Fig. 5.

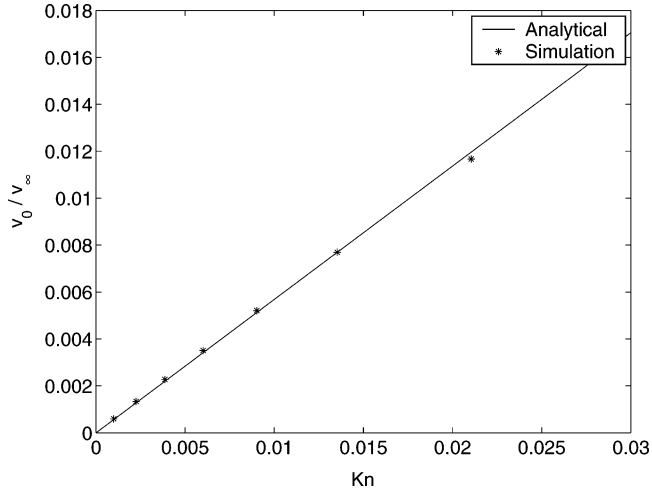

Fig. 3 Relative slip at the wall in the simulation of the Kramers problem for shear rate $a = 0.001$, box length $L = 32$, $v_\infty = a \times L = 0.032$. Figure from [43], computed by S. Ansumali

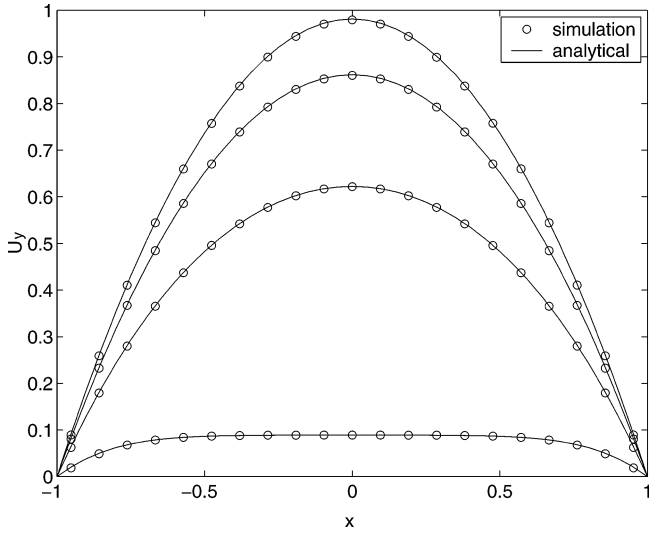

Fig. 4 Development of the velocity profile in the Poiseuille flow. Reduced velocity $U_y(x) = u_y/u_{y_{\max}}$ is shown versus the reduced coordinate across the channel x. Solid line: analytical solution. Different lines correspond to different instants of the reduced time, increasing from bottom to top. Symbol: simulation with the ELBGK algorithm. Parameters used are, viscosity $\mu = 5.0015 \times 10^{-5}$ ($\beta = 0.9997$), steady state maximal velocity $u_{y_{\max}} = 1.10217 \times 10^{-2}$. Reynolds number Re $= 1157$. Figure from [38], computed by S. Ansumali

The essential difference between the lattice Boltzmann and the much earlier main body research on discrete velocity models pioneered by the seminal work of Broadwell [50] is in two points:

- In the lattice Boltzmann, the effort is made on fixing as much as possible of the true (known from continuum theory) Maxwellian dependence of relevant higher-order moments on the hydrodynamic moments with as minimum of discrete velocities as possible, and
- The space-time discretization to allow for large time steps (of the order of the mean free flight rather than of the collision). This is at variance with most of the numerical implementation of discrete velocity models using finite difference ideology.

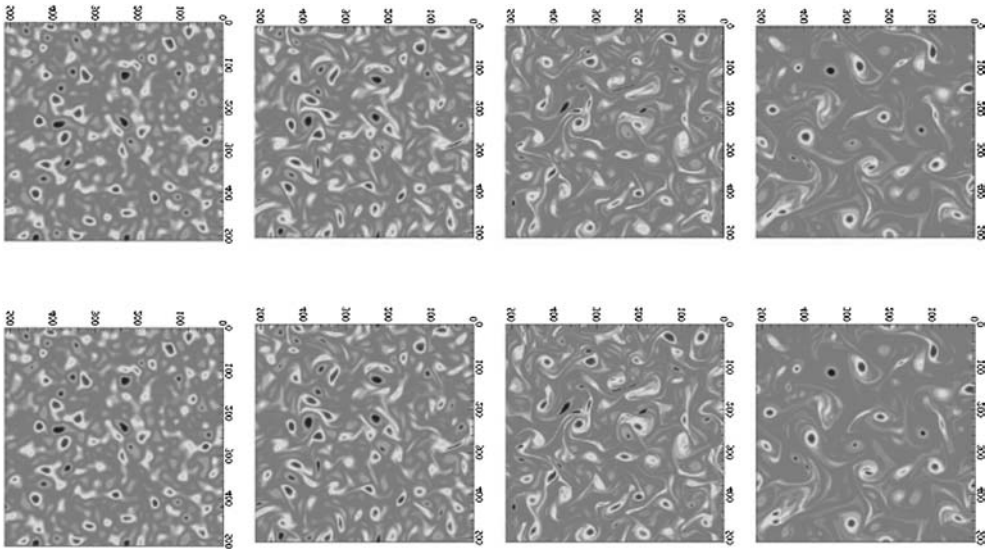

Fig. 5 Snapshots of the vorticity field in the freely decaying $2D$ turbulence at $t = 0$, $t = 1000$, $t = 5000$, $t = 20000$ (from left to right). Time measured in the lattice units. Eddy turnover time $t_{\text{eddy}} \approx 700$. The Reynolds number based on the mean initial kinetic energy E and the box-length L equals $\text{Re} = L\sqrt{2E}/\nu = 13134$. Upper row: spectral method; Bottom row: entropic lattice Boltzmann method. Both computations were performed on the grid of the same size (512×512 grid points). Figure courtesy S. Ansumali

4.8 Outlook: lattice Boltzmann and microflows

Gas flows at the micrometer scale constitute a major portion of contemporary fluid dynamics of engineering interest. Because of its relevance to the engineering of micro electro-mechanical systems (MEMS), the branch of computational fluid dynamics focused on micro scale phenomena is often called "microfluidics" [2, 51]. Microflows are characterized by the Knudsen number, Kn, which is defined as the ratio of the mean free path of molecules λ and the characteristic scale L of variation of hydrodynamic fields (density, momentum, and energy). For typical flows in microdevices, $\text{Kn} \sim \lambda/L$ varies from $\text{Kn} \ll 1$ (almost-continuum flows) to $\text{Kn} \sim 1$ (weakly rarefied flows). Another characteristic property of microflows is that they are highly subsonic, that is, the characteristic flow speed is much smaller than the speed of sound. This feature is characterized by the Mach number, $\text{Ma} \sim u/c_s$, where u is the characteristic flow speed, and c_s is the (isentropic) speed of sound. Thus, for microflows, $\text{Ma} \ll 1$. To be more specific, typical flow velocities are about 0.2 m/s, corresponding to $\text{Ma} \sim 10^{-4}$, while values of the Knudsen number range between $10^{-4} \leq Kn \leq 10^{-1}$. Finally, in the majority of applications, microflows are quasi-two-dimensional.

Theoretical studies of gas flows at finite Knudsen numbers began several decades ago in the realm of the Boltzmann kinetic equation. To this end, we mention pioneering contributions by Cercignani [45], and Sone [52]. These studies focused on obtaining either exact solutions of the stationary Boltzmann kinetic equation, or other model kinetic equations in relatively simple geometries (most often, infinite or semi-infinite rectangular ducts), or asymptotic expansions of these solutions.

While analytical solutions are important for a qualitative understanding of microflows, and also for the validation of numerical schemes, they certainly do not cover all the needs of computational fluid dynamics of practical interest. At present, two CFD strategies for microflows are well established.

- *Equations of continuous fluid mechanics with slip boundary conditions*. The simplest semi-phenomenological observation about microflows is the break down of the no-slip boundary condition of fluid mechanics with increasing Knudsen number. Since microflows are highly subsonic, this leads to the simplest family of models, equations of incompressible or compressible fluid dynamics supplemented by slip velocity boundary conditions (a review can be found in [2]). This approach, although widely used in the early days of microfluidics, remains phenomenological. Moreover, it fails to

predict phenomena such as non-trivial pressure and temperature profiles observed by more microscopic approaches.

- *Direct simulation of the Boltzmann kinetic equation*. On the other extreme, it is possible to resort to a fully microscopic picture of collisions, and to use a molecular dynamics approach or a simplified version thereof – the direct simulation Monte Carlo method of Bird (DSMC) [53]. DSMC is sometimes heralded as the method of choice for simulation of the Boltzmann equation, and it has indeed proven to be robust in supersonic, highly compressible flows with strong shock waves. However, the highly subsonic flows at small to moderate Knudsen number is not a "natural" domain for the DSMC simulations where it becomes computationally intensive [54].

Since semi-phenomenological computations are not reliable, and the fully microscopic treatment is not feasible, the approach to CFD of microflows must rely on reduced models of the Boltzmann equation. Two classical routes of reducing the kinetic equations are well known, the Chapman-Enskog method and Grad's moment method. The Chapman-Enskog method extends the hydrodynamic description (compressible Navier-Stokes equations) to finite Kn in the form of a Taylor series, leading to hydrodynamic equations of increasingly higher order in the spatial derivatives (Burnett's hydrodynamics). Grad's method extends the hydrodynamic equations to a closed set of equations including higher-order moments (fluxes) as independent variables. Both methods are well suited for theoretical studies of microflows. In particular, as was already noted by Grad, moment equations are especially well suited for low Mach number flows.

However, applications of Grad's moment equations or of Burnett's hydrodynamics (or of existing extensions and generalizations thereof) to CFD of microflows are limited at present because of several reasons. The most severe difficulty is in formulating the boundary conditions at the reduced level. Although some studies of boundary conditions for moment systems were initiated recently [55], this problem is far from solved. The crucial importance of the boundary condition for microflows is actually expected. Indeed, as the rarefaction is increasing with Kn, the contribution of the bulk collisions becomes less significant as compared to the collisions with the boundaries, and thus the realistic modelling of the boundary conditions becomes increasingly important.

The entropic lattice Boltzmann method seems to be a promising approach to simulations of microflows, and is currently an active area of research [56–59]. In contrast to Grad's method, ELBM is much more compliant with the boundary conditions (see above the diffusion wall approximation, which was also rediscovered in [60], where ELBM simulations were tested against molecular dynamic simulations with a good agreement). Interested readers are directed to two recent papers [61, 62] where relations between the Grad and the lattice Boltzmann constructions are considered in more detail.

5 Concluding remarks

The aim of this review was to give a birds-eye picture of the method of moments pioneered by Harold Grad a half century ago. Three relatively new issues pertinent to the question of the physics is beyond Grad's moment approximation and how to obtain this physics were discussed in some detail, "Other variables" (triangle entropy method), invariance corrections, and lifting Grad's equations to a kinetic model. We believe that further development of Grad's approach along the lines indicated here will be beneficial to emerging fields of fluid dynamics, and this review "will be of value for both engineers and mathematicians, who may attempt to turn the invariance condition equation into rigorous mathematics", as was suggested by the referee of this paper. As per mathematical rigor, the situation is at least not hopeless for finite-dimensional systems, such as ordinary differential equations of chemical kinetics. However, much more work is needed for infinite-dimensional systems like the Boltzmann equation where the present level of mathematical achievements in such things as existence and uniqueness of solutions does not even allow starting a rigorous discussion on construction of invariant manifolds. Some mathematical requirements are formulated in the recent book [20].

Acknowledgements It is our pleasure to thank Dr. S. Ansumali for his contributions to Sect. 4, and for providing the figures. IVK was supported by the Swiss Federal Department of Energy (BFE) under the project Nr. 100862 "Lattice Boltzmann simulations for chemically reactive systems in a micrometer domain."

References

1. Grad, H.: On the kinetic theory of rarefied gases. Comm. Pure Appl. Math. **2**, 331–407 (1949)
2. Beskok, A., Karniadakis, G.E.: Microflows: Fundamentals and Simulation. Springer, Berlin (2001)
3. Kogan, A.M.: Derivation of Grad-type equations, study of their properties by the method of entropy maximization. Prikl. Math. Mech. **29**, 122–133 (1965)
4. Lewis, R.M.: A unified principle in statistical mechanics. J. Math. Phys. **8**, 1448–1459 (1967)
5. Gorban, A.N.: Equilibrium Encircling. Equations of chemical kinetics, and their thermodynamic analysis. Nauka, Novosibirsk (1984)
6. Karlin, I.V.: Relaxation of chemical reaction rates under translationally nonequilibrium conditions. In: Proc. VIII USSR Symp. on Burning, Combustion, 97–99. Chernogolovka, Inst. Chem. Phys. (1986)
7. Gorban, A.N., Karlin, I.V.: Quasi-equilibrium approximations and non-standard expansions in the theory of the Boltzmann kinetic equation. In: Khlebopros, R.G. (Ed.): Mathematical Modeling in Biology and Chemistry (New Approaches), pp. 69–117. Nauka, Novosibirsk (1991). English translation of the first part of this paper (triangle entropy method): http://arXiv.org/abs/cond-mat/0305599
8. Gorban, A.N., Karlin, I.V.: Scattering rates versus moments: alternative grad equations. Phys. Rev. E **54**, R3109–R3112 (1996)
9. Gorban, A.N., Karlin, I.V.: Thermodynamic parameterization. Physica A **190**, 393–404 (1992)
10. Levermore, C.D.: Moment closure hierarchies. J. Stat. Phys. **83**, 1021 (1996)
11. Ilg, P., Karlin, I.V., Öttinger, H.C.: Canonical distribution functions in polymer dynamics: I. Dilute solutions of flexible polymers. Physica A **315**(3–4), 318–336 (2002)
12. Ilg, P., Karlin, I.V., Kröger, M., Öttinger, H.C.: Canonical distribution functions in polymer dynamics: II. Liquid-crystalline polymers. Physica A **319**, 134–150 (2003)
13. Gorban, A.N., Gorban, P.A., Karlin, I.V.: Legendre integrators, postprocessing and quasiequilibrium. J. Non-Newtonian Fluid Mech. **120**, 149–167 (2004)
14. Müller, I., Ruggeri, T.: Extended Thermodynamics. Springer, Berlin (1993)
15. Bobylev, A.V.: On the Chapman-Enskog and Grad methods. Dokl. Acad. Nauk SSSR **262**, 71 (1982)
16. Karlin, I.V.: Method of Invariant Manifold in Kinetic Theory. PhD thesis, AMSE University, Tassin (1992)
17. Gorban, A.N., Karlin, I.V.: Method of invariant manifolds and regularization of acoustic spectra. Transport Theory and Stat. Phys. **23**, 559–632 (1994)
18. Gorban, A.N., Karlin, I.V.: New Methods for Solving the Boltzmann Equations, vol. 10 [Physical Kinetics] of Scientific Siberian A. AMSE Press, Tassin (1993)
19. Gorban, A.N., Karlin, I.V., Zinovyev, A.Yu.: Constructive methods of invariant manifolds for kinetic problems. Physics Reports **396**, 197–403 (2004)
20. Gorban, A.N., Karlin, I.V.: Invariant Manifolds for Physical and Chemical Kinetics, vol. 660 of Lect. Notes Phys. Springer, Berlin Heidelberg (2005)
21. Gorban, A.N., Karlin, I.V.: Uniqueness of thermodynamic projector and kinetic basis of molecular individualism. Physica A **336**(3–4), 391–432 (2004) Preprint online: http://arxiv.org/abs/cond-mat/0309638
22. Slemrod, M.: Renormalization of the Chapman-Enskog expansion: Isothermal fluid flow, Rosenau saturation. J. Stat. Phys. **91**, 285–305 (1998)
23. Karlin, I.V., Gorban, A.N., Dukek, G., Nonnenmacher, T.: Dynamic correction to moment approximations. Phys. Rev. E **57**, 1668–1672 (1998)
24. Zmievskii, V.B., Karlin, I.V., Deville, M.: The universal limit in dynamics of dilute polymeric solutions. Physica A **275**(1–2), 152–177 (2000)
25. Gorban, A.N., Karlin, I.V.: Structure and approximations of the Chapman-Enskog expansion for Grad linearized equations. Sov. Phys. JETP **73**(4), 637–641 (1991)
26. Struchtrup, H., Torrilhon, M.: Regularization of Grad's 13 moment equations: Derivation, linear analysis. Phys. Fluids **15**, 2668–2680 (2003)
27. Chapman, S., Cowling, T.G.: The Mathematical Theory of Non-Uniform Gases. Cambridge University Press, Cambridge (1970)
28. Gorban, A.N., Karlin, I.V., Zmievskii, V.B., Dymova, S.V.: Reduced description in reaction kinetics. Physica A **275**, 361–379 (2000)
29. Gorban, A.N., Karlin, I.V.: Method of invariant manifold for chemical kinetics. Chem. Eng. Sci. **58**, 4751–4768 (2003)
30. Gorban, A.N., Karlin, I.V., Zinovyev, A.Yu.: Invariant grids for reaction kinetics. Physica A **333**, 106–154 (2004)
31. Gorban, A.N., Karlin, I.V.: Short-wave limit of hydrodynamics: A soluble example. Phys. Rev. Lett. **77**, 282–285 (1996)
32. Karlin, I.V., Gorban, A.N.: Hydrodynamics from Grad's equations: What can we learn from exact solutions? Ann. Phys. (Leipzig) **11**(10–11), 783–833 (2002)
33. Karlin, I.V., Dukek, G., Nonnenmacher, T.: Invariance principle for extension of hydrodynamics: Nonlinear viscosity. Phys. Rev. E **55**(2), 1573–1576 (1997)
34. Santos, A.: Nonlinear viscosity, velocity distribution function in a simple longitudinal flow. Phys. Rev. E **62**, 4747–4751 (2000)
35. Gorban, A.N., Karlin, I.V.: General approach to constructing models of the Boltzmann equation. Physica A **206**, 401–420 (1994)

36. Andries, P., Aoki, K., Perthame, B.: A consistent BGK-type model for gas mixtures. J. Stat. Phys. **106**, 993–1018 (2002)
37. Shan, X., He, X.: Discretization of the velocity space in the solution of the Boltzmann equation. Phys. Rev. Lett. **80**, 65–68 (1998)
38. Ansumali, S., Karlin, I.V.: Entropy function approach to the lattice Boltzmann method. J. Stat. Phys. **107**, 291–308 (2002)
39. Ansumali, S., Karlin, I.V.: Single relaxation time model for entropic lattice Boltzmann methods. Phys. Rev. E **65**(1–9), 056312 (2002)
40. Karlin, I.V., Gorban, A.N., Succi, S., Boffi, V.: Maximum entropy principle for lattice kinetic equations. Phys. Rev. Lett. **81**, 6–9 (1998)
41. Karlin, I.V., Ferrante, A., Öttinger, H.C.: Perfect entropy functions of the lattice Boltzmann method. Europhys. Lett. **47**, 182–188 (1999)
42. Boghosian, B.M., Yepez, J., Coveney, P.V., Wagner, A.J.: Entropic lattice Boltzmann methods. Proc. Roy. Soc. Lond. A **457**, 717–766 (2001)
43. Ansumali, S., Karlin, I.V.: Kinetic boundary condition for the lattice Boltzmann method. Phys. Rev. E **66**(1–6), 026311 (2002)
44. Ansumali, S., Karlin, I.V., Öttinger, H.C.: Minimal entropic kinetic models for simulating hydrodynamics. Europhys. Lett. **63**, 798–804 (2003)
45. Cercignani, C.: Theory and Application of the Boltzmann Equation. Scottish Academic Press, Edinburgh (1975)
46. Ansumali, S., Chikatamarla, S.S., Frouzakis, C.M., Boulouchos, K.: Entropic lattice Boltzmann simulation of the flow past square cylinder. Int. J. Mod. Phys. C **15**(3), 435–445 (2004)
47. Succi, S.: The Lattice Boltzmann Equation for Fluid Dynamics, Beyond. Oxford University Press, Oxford (2001)
48. Karlin, I.V., Ansumali, S., De Angelis, E., Öttinger, H.C., Succi, S.: Entropic lattice Boltzmann method for large scale turbulence simulation. http://xxx.lanl.gov/abs/cond-mat/0306003 (2003)
49. Ansumali, S.: Minimal kinetic modeling of hydrodynamics. PhD thesis, Swiss Federal Inst. of Tech. Zürich, 15534 (2004)
50. Broadwell, J.E.: Study of rarefied shear flow by the discrte velocity method. J. Fluid Mech. **19**, 401–414 (1964)
51. Ho, C.M., Tai, Y.C.: Micro-electro-mechanical-systems(MEMS), fluid flows. Annu. Rev. Fluid Mech. **30**, 579–612 (1998)
52. Sone, Y.: Kinetic Theory, Fluid Dynamics. Birkhäuser, Basel (2002)
53. Bird, G.A.: Molecular Gas Dynamics and the Direct Simulation of gas flows. Theory and Application of the Boltzmann Equation. Clarendon Press, Oxford (1994)
54. Oran, E.S., Oh, C.K., Cybyk, B.Z.: Direct simulation Monte Carlo: Recent advances, applications. Annu. Rev. Fluid Mech. **30**, 403–441 (1998)
55. Grmela, M., Karlin, I.V., Zmievski, V.B.: Boundary layer variational principle: A case study. Phys. Rev. E **66**(1–12), 011201 (2002)
56. Nie, X., Doolen, G., Chen, S.: Lattice-Boltzmann simulations of fluid flows in MEMS. J. Stat. Phys. **107**, 279–289 (2002)
57. Lim, C.Y., Shu, C., Niu, X.D., Chew, Y.T.: Application of lattice Boltzmann method to simulate microchannel flows. Phys. Fluid **107**, 2299–2308 (2002)
58. Succi, S.: Mesoscopic modeling of slip motion at fluid-solid interfaces with heterogeneous catalysis. Phys. Rev. Lett. **89**, 064502 (2002)
59. Li, B., Kwok, D.: Discrete Boltzmann equation for microfluidics. Phys. Rev. Lett. **90**, 124502 (2003)
60. Niu, X.D., Shu, C., Chew, Y.T.: Lattice Boltzmann BGK model for simulation of micro flows. Euro. Phys. Lett. **67**, 600–606 (2004)
61. Ansumali, S., Karlin, I.V., Frouzakis, Ch. E., Boulouchos, K.B.: Entropic lattice Boltzmann method for microflows. http://xxx.lanl.gov/abs/cond-mat/0412555 (2004)
62. Ansumali, S., Frouzakis, Ch. E., Karlin, I.V., Kevrekidis, I.G.: Exploring hydrodynamic closures for the lid-driven micro-cavity. http://arxiv.org/abs/cond-mat/0502018 (2005)